Autoradiographic Analysis of Iodoamphetamine Redistribution in Experimental Brain Ischemia

Hiroshi Matsuda, Shiro Tsuji, Hiroshi Oba, Kazuhiro Shiba, Hitoshi Terada, Keiko Kinuya, Hirofumi Mori, Hisashi Sumiya, and Kinichi Hisada

Department of Nuclear Medicine, School of Medicine, and Radioisotope Center, Kanazawa University, Kanazawa, Japan

The pathophysiologic significance of iodoamphetamine (IMP) redistribution was analyzed using a double radionuclide autoradiography technique in experimental brain ischemia in the rat. Within 4 hr after unilateral arterial occulsion, IMP almost completely redistributed at 150 min postinjection in the affected areas. At 2 min postinjection, both a remarkable decrease of IMP accumulation and histopathologic change of diminished staining were observed in these areas. The redistribution amplitude was higher in the affected hemisphere, especially in the regions surrounding the ischemic core than in the unaffected hemisphere. These findings were consistent with computer simulation studies of the time course of brain activity based on the standard diffusible tracer model. The results suggest that IMP redistribution in the ischemic area is due to differences of the temporal changes of the brain activity between the unaffected and affected areas and that it is a "physical" phenomenon (only flow related) rather than a "biologic" one.

J Nucl Med 1990; 31:660–667

It is well known that N-isopropyl-p-(^{123}I) iodoamphetamine ([^{123}I]IMP) as an agent for brain perfusion imaging shows temporal changes in the distribution pattern in the brain after administration (*1–5*). Late IMP images (3–5 hr postinjection) frequently show a "redistribution" phenomenon that is characterized by the filling-in of the tracer in decreased accumulation areas observed in early IMP images (15–30 min postinjection). We speculate that this redistribution phenomenon is related to metabolic activity in viable cerebral tissue (*1,3,4,6*). However, detailed investigation of the pathophysiologic significance of this phenomenon has not yet been undertaken. We describe here the autoradiographic analysis of this phenomenon in experimental brain ischemia along with computer simulation.

Received Sept. 14, 1989; revision accepted Dec. 21, 1989.

For reprints contact: Hiroshi Matsuda MD, Department of Nuclear Medicine, Kanazawa University School of Medicine, 13-1, Takara-machi, Kanazawa City, 920, Japan.

MATERIALS AND METHODS

Simulation Study

The time course of brain activity after tracer administration was simulated employing the following equation for diffusible tracer model of Kety (*7*):

$$C_b(T) = F[\int_0^T C_a(t)\cdot\exp(-(F/(100\,\lambda))(T-t)dt], \quad (1)$$

where F is the cerebral blood flow in ml/100 g/min, C_a is the arterial whole-blood concentration of true tracer in MBq/ml determined by the octanol extraction technique, C_b is the brain activity concentration in MBq/100 g, t is time, λ is the brain:blood partition coefficient at equilibrium, and T is the time of measurement. The $C_a(t)$ was experimentally measured up to 150 min in a male Sprague-Dawley rat weighing 220 g after administration of 0.37 MBq (10 μCi) of [^{125}I]IMP. The λ was also determined experimentally in the frontoparietal cortices of six male Sprague-Dawley rats weighing 200–250 g by measurement of the concentrations of the tracer in the tissues and in the blood at 150 min postinjection. This time was chosen to achieve equilibrium, as previously reported by Lear et al. (*8*). Using these experimental data and a microcomputer (NEC PC-9801, Tokyo, Japan), the $C_b(t)$ was generated relative to varying cerebral blood flow values at intervals of 2 min for the first 30 min and then every 15 min from 45 to 150 min. Integrals were calculated by numerical integration using a spline approximation.

Autoradiographic Study

Animals and experimental procedures. Ten male Sprague-Dawley rats weighing 200–250 g were permitted free access to food and water before the experiment. The animals were anesthetized with halothane (1–1.5%). Using Tamura's method (*9,10*), an unilateral middle cerebral artery was pinched with a small Zen clip (Ohwa Tsusho Co. Ltd., Tokyo, Japan). The femoral arteries and veins were cannulated with polyethylene catheters for administration of radioactive tracers and for measurements of arterial blood pressure, pH, Pa_{CO_2}, and Pa_{O_2}.

One hour after the occulsion of the middle cerebral arteries, 1.85 MBq (50 μCi) of [^{125}I]IMP (100% ^{125}I radionuclide purity, Nihon Medi-Physics, Takaradzuka, Japan) was intravenously

injected. One hundred and forty eight minutes postinjection of [^{125}I]IMP, 55.5 MBq (1.5 mCi) of [^{123}I]IMP, Nihon Medi-Physics, Takaradzuka, Japan) was infused intravenously for 30 sec. The ^{123}I used here was produced by the process: ^{127}I(p,5n)^{123}Xe→^{123}I. This reaction also produces less than 4.5% ^{125}I contamination. Twelve 0.03-ml arterial blood samples were withdrawn at ~7-sec intervals during the first 1 min and at ~20-sec intervals during the second minute. Unmetabolized [^{123}I]IMP was extracted from the collected arterial samples using the octanol extraction technique, as previously reported (*11*). The animals were killed by decapitation 2 min after the start of the injection of [^{123}I]IMP, that is, 150 min after the injection of [^{125}I]IMP. The brain was quickly removed and frozen at −70°C in hexan-dry ice. Sections (20 μm thick) were cut at −20°C with a cryostat, mounted on coverslips, and dried for autoradiography. The first exposure was carried out for 36 hr to obtain [^{123}I]IMP images. Ten days later (18 half-lives of ^{123}I) when [^{123}I]IMP activity was negligible, the second exposure, lasting for 2 mo, was carried out to obtain [^{125}I]IMP images.

From 0.11 to 1.18 MBq/g (3 to 32 μCi/g) of [^{123}I]IMP, which was prepared from the same batch of [^{123}I]IMP as that administered to the animals, was mixed with 0.2 g gelatin and 1.0 ml distilled water, and heated to 60°C until the gelatine dissolved to make the autoradiography standards for ^{123}I. The standard was frozen in the same manner as for the brain sections. Half of it was sliced in a cryostat into 20 μm thick sections which exposed x-ray films (Sakura A type, Tokyo) in x-ray cassettes along with brain tissue slices in both the first and second exposures. The other half was assayed for radioactivity in a gamma scintillation counter to obtain the ^{123}I concentration in MBq/g.

In five rats, adjacent 20-μm brain slices were stained with hematoxylin and eosin to evaluate neuropathologic changes.

Data analysis of autoradiograms. Autoradiograms were processed with a microcomputer-based solid state image analyzer as previously reported (*11*), by which optical densities were converted to digital numbers. The following theory is derived to obtain independent early (2 min postinjection) and late (150 min postinjection) IMP images for each section.

The first exposure for brain sections is formed by the action of ^{123}I and ^{125}I:

$$E_{b1} = {}^{123}I_{b1} + {}^{125}I_{b1}' + {}^{125}I_{b1}, \quad (2)$$

where E_{b1} = exposure from tissue section in the first exposure, $^{123}I_{b1}$ = exposure component of E_{b1} contributed by ^{123}I of [^{123}I] IMP, $^{125}I_{b1}'$ = exposure component of E_{b1} contributed by the contaminant ^{125}I of [^{123}I]IMP, and $^{125}I_{b1}$ = exposure component of E_{b1} contributed by ^{125}I of [^{125}I]IMP.

Since the second exposure was carried out after a suitable period for ^{123}I decay, the second exposure is formed by the action of only ^{125}I:

$$E_{b2} = {}^{125}I_{b2}' + {}^{125}I_{b2}, \quad (3)$$

where E_{b2} = exposure from tissue section in the second exposure, $^{125}I_{b2}'$ = exposure component of E_{b2} contributed by the contaminant ^{125}I of [^{123}I]IMP, and $^{125}I_{b2}$ = exposure component of E_{b2} contributed by ^{125}I of [^{125}I]IMP.

The first exposure for standard sections prepared from [^{123}I] IMP is formed by the action of ^{123}I and ^{125}I:

$$E_{s1} = {}^{123}I_{s1} + {}^{125}I_{s1}', \quad (4)$$

where, E_{s1} = exposure from standard section in the first exposure, $^{123}I_{s1}$ = exposure component of E_{s1} contributed by ^{123}I of [^{123}I]IMP, and $^{125}I_{s1}'$ = exposure component of E_{s1} contributed by the contaminant ^{125}I of [^{123}I]IMP.

The second exposure for standard sections after a suitable period for ^{123}I decay is formed by the action of only ^{125}I:

$$E_{s2} = {}^{125}I_{s2}', \quad (5)$$

where, E_{s2} = exposure from standard section in the second exposure, $^{125}I_{s2}'$ = exposure component of E_{s2} contributed by the contaminant ^{125}I of [^{123}I]IMP.

Since brains and gelatin standards are labeled with ^{123}I from the same batch, the amount of ^{125}I impurity in the brain and standard sections is equal:

$$\alpha = E_{s2}/E_{s1} = {}^{125}I_{s2}'/({}^{123}I_{s1} + {}^{125}I_{s1}') = {}^{125}I_{b2}'/({}^{123}I_{b1} + {}^{125}I_{b1}'), \quad (6)$$

where α = ratio of the contaminant ^{125}I exposure in E_{b2} or E_{s2} to ^{123}I and the contaminant ^{125}I exposure in E_{b1} or E_{s1}. In Equation 2, $^{125}I_{b1}$ was estimated at <3% of E_{b1} from the observation of [^{125}I]IMP gelatin standards of 5.6 to 59.2 KBq/g (0.15 to 1.6 μCi/g) exposure on a x-ray film for 36 hr. Therefore:

$$E_{b1} = {}^{123}I_{b1} + {}^{125}I_{b1}' + {}^{125}I_{b1} \fallingdotseq {}^{123}I_{b1} + {}^{125}I_{b1}'. \quad (7)$$

Substituting Equation 7 to Equation 6 yields:

$$\alpha = {}^{125}I_{b2}/E_{b1} \quad (8)$$

Substituting arranged Equation 8 to Equation 3 gives:

$$E_{b2} = \alpha \cdot E_{b1} + {}^{125}I_{b2}. \quad (9)$$

Thus:

$$\text{Early IMP image} = E_{b1} \quad (10)$$

and

$$\text{Late IMP image} = {}^{125}I_{b2} = E_{b2} - \alpha \cdot E_{b1}, \quad (11)$$

where α values are obtainable from the E_{s2}/E_{s1} ratio for [^{123}I] IMP gelatin standards, as mentioned above. An image subtraction technique was used on a pixel-by-pixel basis to obtain the late IMP images after precise superimposition of the first and second autoradiograms from the same brain slice.

Local cerebral blood flow (LCBF) values were determined in early IMP images, as previously reported (*11*). The energy window of a gamma scintillation counter was set to 111−207 keV to eliminate the ^{125}I activity of [^{125}I]IMP. This setting also eliminates the contaminant ^{125}I activity of [^{123}I]IMP; however, global overestimation of flow values due to this elimination is estimated at < 4%.

Redistribution index images were made after the normalization of early and late IMP images as follows:

$$E_n = 100\ (\text{Early IMP image} - \text{BKG})/(\text{Max.} - \text{BKG}) \quad (12)$$

$$L_n = 100\ (\text{Late IMP image} - \text{BKG})/(\text{Max.} - \text{BKG}) \quad (13)$$

$$\text{Redistribution Index image} = 100 + L_n - E_n, \quad (14)$$

where E_n and L_n represent normalized early and late IMP

images respectively, BKG is a digital number of background density, and Max. is the maximal digital number of density in each autoradiogram. The greater the redistribution index in a particular brain region becomes, the greater is the redistribution seen in the region.

The overall relationship between redistribution indexes and cerebral blood flow values was investigated. For each pixel, a redistribution index and cerebral blood flow value were generated, which resulted in a plot containing ~17,000 points for each section compared. Two representative sections for each animal were compared in this manner and the results were summed, yielding a final plot with ~340,000 points. Finally the results from all animals were summed and plots containing mean redistribution indexes and standard deviations were generated from the redistribution index versus cerebral blood flow value by the microcomputer using the technique of Lear et al. (*12*).

Chromatographic Study

A thin-layer chromatographic technique was developed to investigate what substance redistributes in ischemic areas. Two male Sprague-Dawley rats with occulsion of unilateral middle cerebral arteries were administered 37 MBq (1 mCi) of [^{123}I] IMP by tail-vein injection. At 150 min postinjection, the animals were killed by decapitation. The brains were quickly removed and frontoparietal cortexes in both affected and unaffected hemispheres were separately homogenized with 5 ml of 0.32 *M* sucrose. Small aliquots of the homogenates were spotted onto Merck silica-gel strips along with control samples of [^{123}I]IMP. The strips were developed in a 85/14/1 mixture of $CHCl_3$/MeOH/AcOH. The strips were then cut into 5 mm long sections and counted in a gamma scintillation counter.

RESULTS

Simulation Study

The time course of true IMP activity of whole arterial blood in a rat is shown in Figure 1. The obtained values for λ were 15 ± 2 (mean ± s.d.). Setting the λ value to 15 or 7.5 and introducing the obtained whole arterial blood activity of true tracer to Eq. 1 generated simulation curves of the time course of brain activity relative to varying flow values (Fig. 2). The brain activities directly correlate with the cerebral blood flow values at 2 min postinjection; however, at 150 min postinjection, brain activities are essentially dependent on λ values with nearly equal values above the flow level of 30 to 40 ml/100g/min for each λ value.

Autoradiographic Study

Immediately after arterial occulsion, all animals developed some degree of neurologic deficit. Physiologic variables were within physiologic limits; mean arterial blood pressure, 118 ± 5 mmHg; pH, 7.37 ± 0.01; Pa_{CO_2}, 35.2 ± 0.8 mmHg; Pa_{O_2}, 92.1 ± 2.4 mmHg.

Independent early and late IMP images were obtained after the digital processing of the autoradiograms. The mean value of α was 1.07. Representative color-coded images for early IMP, late IMP, redistribution index, and hematoxylin eosin staining are shown in Figure 3. The early IMP image showed remarkably decreased uptake in the cerebral cortex of the lateral convexity and the lateral segment of the caudate putamen ipsilateral to the occulsion. On the other hand, although the areas with diminished staining were observed in a part of the cerebral cortex and the lateral segment of the caudate putamen, the late IMP image showed no significant focally decreased accumulation in the affected hemisphere, which indicates almost complete redistribution in the affected hemisphere. The redistribution index image revealed that IMP predominantly redistributes in the affected hemisphere especially in the areas surrounding the ischemic core. Over-

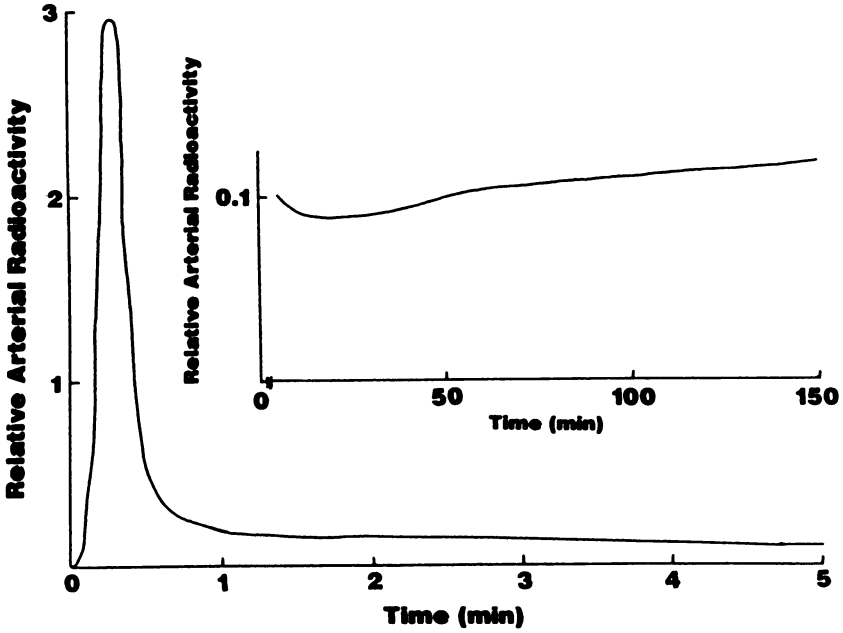

FIGURE 1
Time course of relative true IMP activity of whole arterial blood in a rat up to 150 min postinjection.

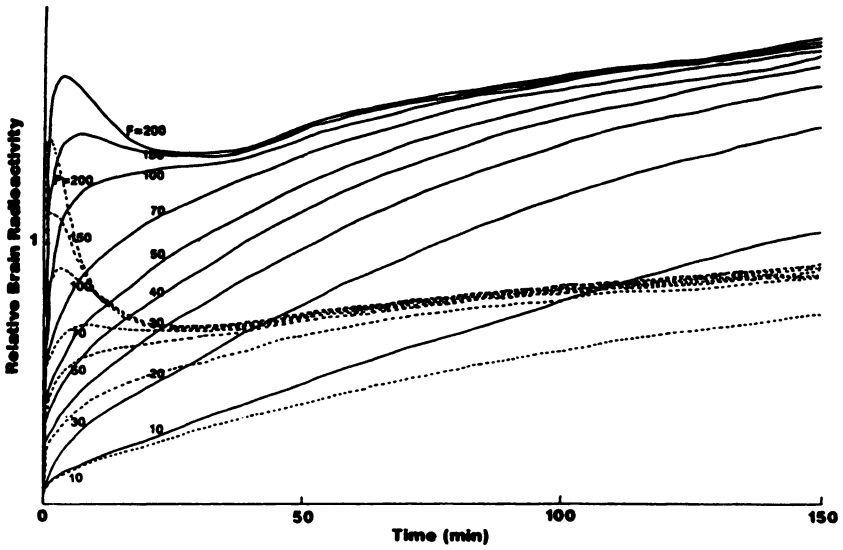

FIGURE 2
Computer simulation of time course of relative brain IMP activity relative to varying cerebral blood flow values (F) in ml/100 g/min when λ is 15 (solid lines) or 7.5 (dashed lines).

all relationships between IMP redistribution indices and cerebral blood flow values (Fig. 4) disclosed a gentle peak of the indices at flow values of ~30 to 50 ml/100 g/min, with IMP redistributing less as the flow value increases above this level.

Chromatographic Study

Thin layer chromatograms for IMP control and brain homogenates of the affected and unaffected cortices are shown in Figure 5. IMP control showed a peak at Rf of 0.53. Brain homogenates at 150 min postinjection showed quite similar patterns between the affected and unaffected cortices with two peaks at Rf of 0.23 and 0.53.

DISCUSSION

In this simulation study, IMP kinetics in the brain are assumed to follow the standard diffusible tracer model with two compartments of blood and brain tissue. It is reported that IMP is rapidly dealkylated to a lipophilic metabolite of p-iodoamphetamine (PIA) in the brain (*13,14*). No other metabolites have been found in the presence of an intact blood-brain barrier (BBB). Rapin et al. (*15*) reported that the kinetics of this metabolite exhibit practically no significant differences from those of IMP in the brain. Both IMP and PIA are avidly taken up in the brain and slowly eliminated from it. These results suggest that IMP acts like a metabolically inert flow tracer such as xenon-133 for

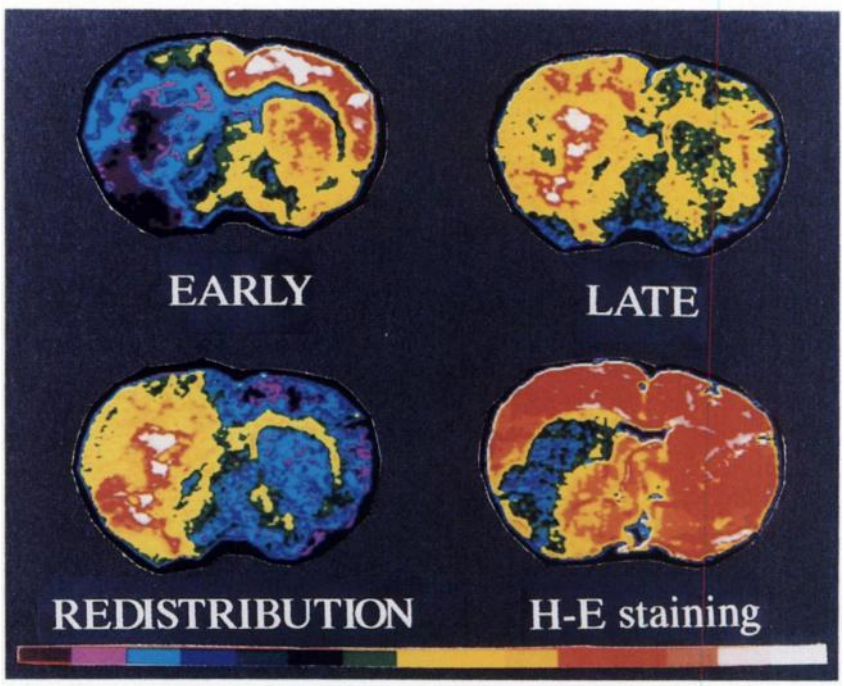

FIGURE 3
Color-coded images for representative early IMP, late IMP, redistribution index, and hematoxylin and eosin staining in experimental brain ischemia in the rat.

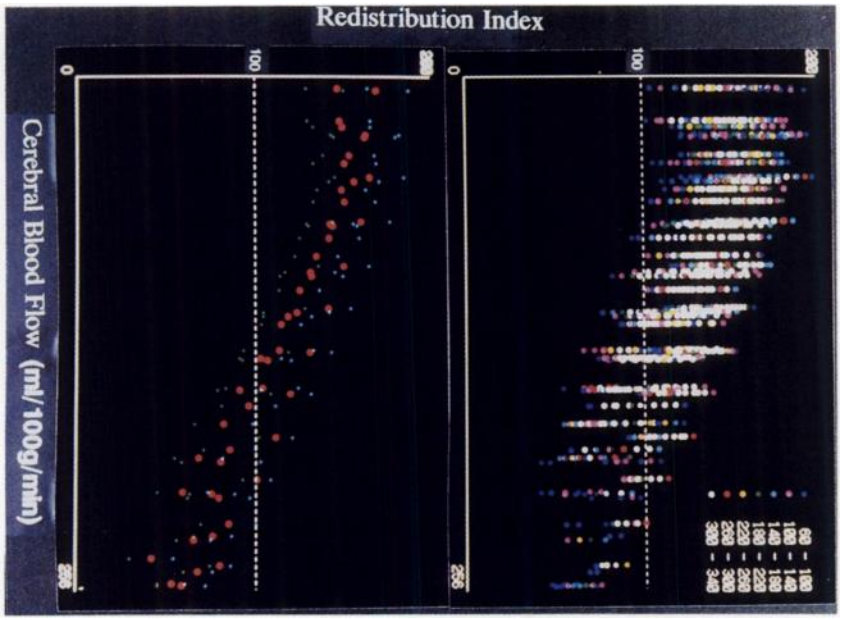

FIGURE 4
Overall relationship between redistribution index and cerebral blood flow values. Upper: Pairs of a redistribution index and flow value are plotted for ~340,000 pixels. Point color indicates the overlap number with a maximum value of 340. Lower: The mean values (red dots) are plotted with 1 s.d. (blue and green dots).

several hours postinjection. Thus, IMP kinetics are considered to be mathematically regulated by two independent factors, flow and the partition coefficient between blood and brain tissue. The individual effects of flow (F) and partition coefficient (λ) on brain activity (Cb) are mathematically demonstrated by taking the differential of Cb with the values for F and λ as independent variables as a function of measurement time (T):

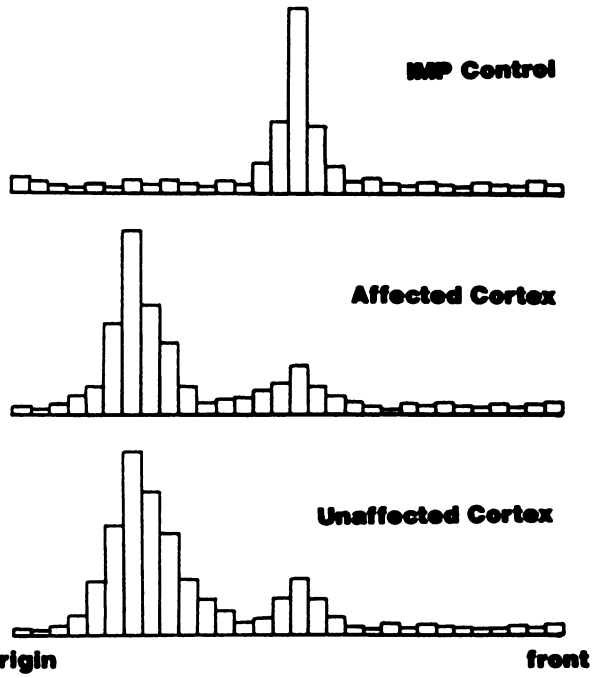

FIGURE 5
Chromatographic profile of IMP control and brain homogenates from affected and unaffected cortices.

$$\frac{dCb}{Cb} = \frac{F}{Cb}\frac{\partial Cb(F,T)}{\partial F}\frac{dF}{F}. \quad (15)$$

$$\frac{dCb}{Cb} = \frac{\lambda}{Cb}\frac{\partial Cb(\lambda,T)}{\partial \lambda}\frac{d\lambda}{\lambda}. \quad (16)$$

Setting the values for F and λ to 150 ml/100 g/min and 15, respectively (Fig. 6), the effect on Cb of the change in the value of F is initially profound postinjection; it is, however, almost negligible beyond 1 hr postinjection. On the other hand, Cb is dependent only on the change in the value of λ after 1 hr.

Chromatographic analysis revealed the presence of the same metabolite in the ischemic areas as in the unaffected areas, which would indicate redistribution of PIA in the ischemic areas. Accordingly, this two compartmental analysis is also applicable to the ischemic areas. To eliminate the influence of BBB destruction, we chose a model of acute brain ischemia within 4 hr after arterial occulsion in this study. Under the BBB destruction, circulating polar metabolites of IMP such as p-iodobenzoic acid that normally do not cross the BBB can modify the IMP distribution in the brain (*16*). Blood-brain barrier destruction is reported not to occur during the initial 4 hr after arterial occulsion (*17,18*).

To our knowledge the combination of the two radionuclides, ^{123}I and ^{125}I, has not been used for multiple tracer autoradiography, possibly because of the difficulty in eliminating the influence of a contaminant in ^{123}I produced by cyclotron. Four percent contamination of ^{125}I in 55.5 MBq (1.5 mCi) of ^{123}I results in 2.2 MBq (60 μCi) of ^{125}I, which is almost equal to the injection dose of [^{125}I]IMP. Consequently, the contribution of contaminant ^{125}I of [^{123}I]IMP to the autoradiograms is almost identical to that of [^{125}I]IMP in the second

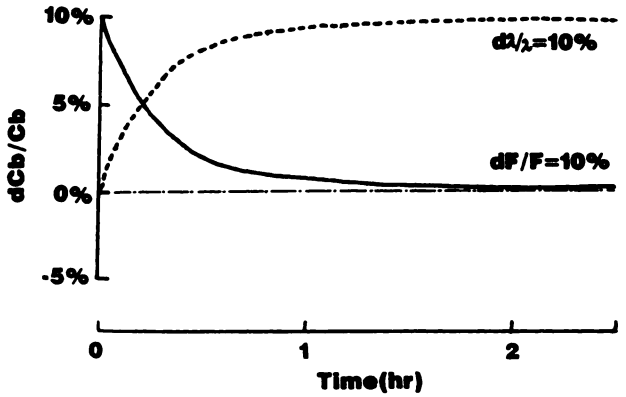

FIGURE 6
The percent effect on brain activity (dCb/Cb) owing to 10% change in the value for flow (dF/F) and λ (d λ/λ) as a function of time.

exposure. However, precise registration of the first and second autoradiograms and the use of autoradiographic standards to correct for cross-contamination enabled us to extract only [^{125}I]IMP distribution from the second autoradiograms using a computer-assisted image subtraction technique. This double radionuclide technique made it possible to evaluate alterations of the tracer distribution at two times after the administration in autoradiography. One of the disadvantages of the autoradiographic technique had been the fact that a single temporal image of the tracer distribution could be obtained. However, recently this drawback has been overcome with the use of two radiolabeled forms of a tracer (*19,20,21*) or the use of the two kinds of tracers with similar characteristics (*22*). This sequential administration technique has widened the application of autoradiography. Obrenovitch et al. (*21*) reported the alternative combination of two radionuclides for IMP, namely that of ^{131}I and ^{125}I. This combination, however, required that the duration for the first exposure and the waiting interval to allow the full decay of ^{131}I till the second exposure be much longer than the combination used here. The longer duration for the first exposure worsens the purity of the first autoradiogram because of cross-contamination by ^{125}I. Moreover, ^{131}I autoradiography has poor resolution (*23*). Because of its high energy, little auto-absorption within the tissue section occurs and thus results in appreciable scatter. Recently, ^{123}I has been produced by the process: ^{124}Xe(p,2n)^{123}I (Nihon Medi-Physics, Takaradzuka, Japan). This reaction produces < 0.3% tellerium-123 contamination. The use of this new [^{123}I]IMP could make the double radionuclide autoradiography technique much easier in the future than the presented one in this study.

Late IMP images revealed the prominent filling-in of IMP in the ischemic areas demonstrated in early IMP images, where the activities in the affected areas are almost equivalent to or partly surpass those in the unaffected areas. Redistribution index images showed a high redistribution amplitude in the affected hemisphere selectively in the surrounding areas of the ischemic core. This finding is also confirmed in the overall relationship between the redistribution indices and cerebral blood flow values. The mathematical λ may be physiologically related to the retention of IMP in the brain tissue as shown in Figure 6. The low λ values result in low brain activities at 150 min postinjection as shown in Figure 2. Consideration of both the autoradiographic and simulation results leads to the assumption that IMP retention in brain tissue does not deteriorate in the ischemic areas. As shown in the computer simulation of the time course of brain activity at various blood flow levels, when the flow value is above 30 to 40 ml/100g/min, brain activities become almost equal at 150 min postinjection. Even below this flow level there is a possibility that brain activity reaches the same level after 150 min insofar as the λ value is preserved. These results suggest that the redistribution phenomenon of IMP visually inspected from the early and late images is due to the co-existence of different time courses of brain activity among brain regions that have different flow levels with similar retentivity for IMP. High flow areas have a steeper initial increase and a subsequent milder increase in brain activities than low flow areas as shown in Figure 2.

The lung plays an important role in the manifestation of this redistribution phenomenon. Immediately after the injection, the lung accumulates almost 100% of IMP (*24,25*). Thereafter, IMP is washed out from the lung, which acts as a reservoir of IMP for the input to the brain for a long period postinjection. Besides, IMP is not converted to polar metabolites in the blood cells (*26*) unlike other technetium-99m- (^{99}mTc) labeled flow tracers, ^{99m}Tc-hexamethyl-propyleneamine oxime (*27*) or ^{99m}Tc-ethyl-cysteinate dimer (*28*). These characteristics of IMP kinetics are also speculated from the time course of arterial blood activity shown in Figure 1. Lipophilic tracer activity is observed over a long time postinjection in the arterial blood with some increase from 20 min. Thus, a considerable amount of lipophilic tracer recirculates to the brain over a long period.

The retention mechanism of IMP in brain tissue has not been clarified, but Winchell et al. (*29*) reported that IMP binds to high-capacity, relatively nonspecific amine binding sites. This was experimentally verified using an in vitro binding assay in our report (*30*). We showed the presence of saturable binding of IMP with an apparent dissociation constant, K_d of 56 μM, and an estimated maximum number of binding sites, B_{max} of 15.7 nmol/mg protein in the rat brain. This remarkably high capacity of IMP binding sites is consistent with the occurrence of the redistribution phenomenon. Selective tissue necrosis was reported in the 2 hr middle cerebral artery occulsion model in monkeys (*31*). Tamura et al. reported irreversible ischemic damage with

morphologic characteristics in the affected areas 2 hr after arterial occulsion in this model (*9*), which was confirmed by hemotoxilin and eosin staining in the present study. Even if a large number of the IMP binding sites are damaged due to ischemic insult, the remaining binding sites may be sufficient to retain IMP because of the quite small chemical dose of the injected IMP as long as there is not total necrosis of brain tissue. This suggests that the late IMP images, which would reflect IMP retention, are not related to brain function. Our preliminary report (*32*) comparing IMP redistribution and brain metabolism, or the report on the relationship between IMP redistribution and cerebral oxygen metabolism measured by positron emission tomography (*33*) may support this hypothesis. From these results, IMP retention in brain tissue is speculated to be not so susceptible to ischemic insult. Further investigation is, of course, necessary to clarify the alteration of IMP binding sites under ischemic conditions. Also, caution must be exerted when directly applying these results in acute experimental ischemia to the clinical findings in the human brain. Nevertheless, the autoradiographic results were consistent with those from the simulation study and help to explain the redistribution phenomenon.

The results suggest that there is an apparent redistribution "filling in" of IMP in ischemic areas. The redistribution is more pronounced in ischemic than in normal areas. The mechanisms responsible for IMP retention are not affected by ischemic insult. Initial differences between early images of the normal and ischemic areas appear to be related to differences in flow. However, at later time points, late images show comparable concentrations in normal and ischemic regions, suggesting eventual "filling in" of the lower flow regions (ischemic regions). Computer simulation suggests that the "filling in" effect in the ischemic area is more related to residual flow (F) than changes of partition coefficient (λ). The initial high lung uptake of IMP may serve as a reservoir for "redistribution." In conclusion, the IMP redistribution is a "physical" phenomenon (only flow related) rather than a "biologic" one.

ACKNOWLEDGMENTS

This work was supported by the Grant-In-Aid for Encouragement of Young Scientists, 01770774, the Ministry of Education, Science and Culture.

The authors thank Nihon Medi-Physics for the gift of the IMP used in this study and Mr. John Gelbrum for proofreading.

REFERENCES

1. Creutzig H, Schober O, Gielow P, et al. Cerebral dynamics of N-isopropyl-(^{123}I)-p-iodoamphetamine. *J Nucl Med* 1986; 27:178–183.
2. Raynaud C, Rancurel G, Samson Y, et al. Pathophysiologic study of chronic infarcts with I-123 isopropyl iodo-amphetamine (IMP): the importance of periinfarct area. *Stroke* 1987; 18:21–29.
3. Moretti JL, Cinotti L, Cesaro P, et al. Amines for brain tomoscintigraphy. *Nucl Med Commun* 1987; 8:581–595.
4. Defer G, Moretti JL, Cesaro P, et al. Early and delayed SPECT using N-isopropyl p-iodoamphetamine iodine-123 in cerebral ischemia. *Arch Neurol* 1987; 44:715–718.
5. Nishizawa S, Tanada S, Yonekura Y, et al. Regional dynamics of N-isopropyl-(^{123}I)p-iodoamphetamine in human brain. *J Nucl Med* 1989; 30:150–156.
6. Ackerman RH. Of cerebral blood flow, stroke and SPECT. *Stroke* 1984; 15:1–4.
7. Kety SS. The theory and applications of the exchange of inert gas at the lungs and tissues. *Pharmacol Rev* 1951; 3:1–41.
8. Lear JL, Ackermann RF, Kameyama M, et al. Evaluation of [^{123}I]isopropyliodoamphetamine as a tracer for local cerebral blood flow using direct autoradiographic comparison. *J Cereb Blood Flow Metabol* 1982; 2:179–185.
9. Tamura A, Graham DI, McCulloch J, et al. Focal cerebral ischemia in the rat: 1. description of technique and early neruopathological consequences following middle cerebral artery occulsion. *J Cereb Blood Flow Metabol* 1981; 1:53–60.
10. Tamura A, Graham DI, McCulloch J, et al. Focal cerebral ischaemia in the rat: 2. regional cerebral blood flow determined by [^{14}C]iodoantipyrine autoradiography following middle cerebral artery occulsion. *J Cereb Blood Flow Metabol* 1981; 1:61–69.
11. Matsuda H, Tsuji S, Oba H, et al. Direct autoradiographic comparison of ^{99m}Tc-HMPAO with ^{125}I-IMP in experimental brain ischaemia. *Nucl Med Commun* 1988; 9:891–897.
12. Lear JL. Quantitative local cerebral blood flow measurements with technetium-99m HM-PAO: evaluation using multiple radionuclide digital quantitative autoradiography. *J Nucl Med* 1988; 29:1387–1392.
13. Rapin JR, Duterte D, Le Poncin-Lafitte M, et al. Iodoamphetamine derivatives as tracers for cerebral blood flow or not? Autoradiographic and autohistoradiographic studies [Abstract]. *J Cereb Blood Flow Metabol* 1983; 3(suppl 1):S105–S106.
14. Baldwin RM, Wu JL. In vivo chemistry of lofetamine HCl iodine-123 (IMP). *J Nucl Med* 1988; 29:122–124.
15. Rapin JR, Le Poncin-Lafitte M, Duterte D, et al. Iodoamphetamine as a new tracer for local cerebral blood flow in the rat: comparison with isopropyliodoamphetamine. *J Cereb Blood Flow Metabol* 1984; 4:270–274.
16. Raynaud C, Rancurel G, Tzourio, et al. SPECT analysis of recent cerebral infarction. *Stroke* 1989; 20:192–204.
17. Olsson Y, Crowell RM, Klatzo I. The blood-brain barrier to protein tracers in focal cerebral ischemia and infarction caused by occlusion of the middle cerebral artery. *Acta Neuropathol (Berl)* 1971; 18:89–102.
18. Hossman KA, Schuier FJ. Metabolic (cytotoxic) type of brain edema following middle cerebral artery occulsion in cats. In: Price TR, Nelson E, eds. *Cerebrovascular diseases*. New York: Raven Press; 1979:141–165.
19. Olds JL, Frey KA, Ehrenkaufer RL, et al. A sequential double-label autoradiographic method that quantifies altered rates of regional glucose metabolism. *Brain Res* 1985; 361:217–224.
20. Redies C, Diksic M, Evans AC, et al. Double-label autoradiographic deoxyglucose method for sequential measurement of regional cerebral glucose utilization. *Neuroscience* 1987; 22:601–619.
21. Obrenovitch TP, Clayton CB, Strong AJ. A double-radionuclide autoradiographic method using N-isopropyl-iodoamphetamine for sequential measurements of local cerebral blood flow. *J Cereb Blood Flow Metabol* 1987; 7:356–365.

22. Matsuda H, Tsuji S, Oba H, et al. Double tracer autoradiographic method for sequential evaluation of regional cerebral perfusion. *Am J Physiol Imaging* 1990; 4:131–135.
23. Mies G, Niebuhr I, Hossman KA. Simultaneous measurement of blood flow and glucose metabolism by autoradiographic techniques. *Stroke* 1981; 5:581–588.
24. Holman BL, Lee RGL, Hill TC, et al. A comparison of two cerebral perfusion tracers, N-isopropyl I-123 p-iodoamphetamine and I-123 HIPDM, in the human. *J Nucl Med* 1984; 25:25–30.
25. Rahimian J, Glass EC, Touya JJ, et al. Measurement of metabolic extraction of tracers in the lung using a multiple indicator dilution technique. *J Nucl Med* 1984; 25:31–37.
26. Kuhl DE, Barrio JR, Huang S-C, et al. Quantifying local cerebral blood flow by N-isopropyl-p-[^{123}I]iodoamphetamine (IMP) tomography. *J Nucl Med* 1982; 23:196–203.
27. Neirinckx RD, Canning LR, Piper IM, et al. Technetium-99m-d,l,-HM-PAO: a new radiopharmaceutical for SPECT imaging of regional cerebral blood perfusion. *J Nucl Med* 1987; 28:191–202.
28. Vallabhajosula S, Zimmerman RE, Picard M, et al. Technetium-99m ECD: a new brain imaging agent: in vivo kinetics and biodistribution studies in normal human subjects. *J Nucl Med* 1989; 30:599–604.
29. Winchell HS, Horst WD, Braun L, et al. N-isopropyl-[^{123}I]p-iodoamphetamine: single-pass brain uptake and washout; binding to brain synaptosomes; and localization in dog and monkey brain. *J Nucl Med* 1980; 21:947–952.
30. Mori H, Shiba K, Tsuji S, et al. Binding sites and subcellular distribution of N-isopropyl-p-(I-125) iodoamphetamine in the rat brain. *Jpn J Nucl Med (Kaku-Igaku)* 1986; 23:1585–1594.
31. Marcoux FW, Mrawetz RB, Crowell RM, et al. Differential regional vulnerability in transient focal cerebral ischemia. *Stroke* 1982; 13:339–346.
32. Oba H, Matsuda H, Tsuji S, et al. Relationship between IMP redistribution and metabolism in experimental brain ischemia [Abstract]. *J Cereb Blood Flow Metabol* 1989; 9(suppl 1):S423.
33. Nishizawa S, Yonekura Y, Tanada S, et al. Value and limitation of early and late SPECT of I-123 IMP in CVD: comparison with PET measurement of cerebral blood flow and oxygen metabolism [Abstract]. *J Nucl Med* 1988; 29:844.